atmosphere

MDPI

Article

Temporal Dynamics of CO_2 Fluxes Measured with Eddy Covariance System in Maize, Winter Oilseed Rape and Winter Wheat Fields

Robert Czubaszek * and Agnieszka Wysocka-Czubaszek

Faculty of Civil Engineering and Environmental Sciences, Bialystok University of Technology, Wiejska 45A Str., 15-351 Bialystok, Poland

* Correspondence: r.czubaszek@pb.edu.pl

Abstract: The full understanding of variation and temporal changes in carbon dioxide (CO_2) fluxes in cropland may contribute to a reduction in CO_2 emissions from agriculture. The aim of this study was to determine the CO_2 exchange intensity in the three most popular crops in Poland. The CO_2 fluxes in summer maize, winter oilseed rape and winter wheat fields were measured using the eddy covariance system. The seasonal dynamics of CO_2 fluxes for all studied crops varied from each other due to individual dynamics in atmospheric CO_2 assimilation of each species through the growing season. The weighted average values of CO_2 fluxes calculated for the entire vegetation period were −22.22 μmol CO_2 m^{-2} s^{-1}, −14.27 μmol CO_2 m^{-2} s^{-1} and −11.95 μmol CO_2 m^{-2} s^{-1} for maize, oilseed rape and wheat, respectively. All the studied agro-ecosystems were carbon sinks during the growing season. The highest negative values of CO_2 fluxes (−36.31 μmol CO_2 m^{-2} s^{-1} and −33.56 μmol CO_2 m^{-2} s^{-1}) were observed in the maize field due to the high production of biomass. However, the maize field was also the most significant carbon source due to slow growth of plants at the beginning of the growing season, and due to leaving the field fallow after harvest until the next sowing. In these two periods, the CO_2 fluxes ranged from 0.59 μmol CO_2 m^{-2} s^{-1} to 3.72 μmol CO_2 m^{-2} s^{-1}. CO_2 exchange over wheat and oilseed rape fields was less intense, but more even throughout the growing season. In the wheat field, the CO_2 fluxes ranged from −1.70 μmol CO_2 m^{-2} s^{-1} to −23.49 μmol CO_2 m^{-2} s^{-1} and in the oilseed rape field they ranged from −1.40 μmol CO_2 m^{-2} s^{-1} to −22.08 μmol CO_2 m^{-2} s^{-1}. In addition, the catch crop in the oilseed rape field contributed to the intensive absorption of CO_2 after harvesting the main crop.

Keywords: CO_2 fluxes; eddy covariance; plant development stage; maize field; winter oilseed rape field; winter wheat field; cropland

Citation: Czubaszek, R.; Wysocka-Czubaszek, A. Temporal Dynamics of CO_2 Fluxes Measured with Eddy Covariance System in Maize, Winter Oilseed Rape and Winter Wheat Fields. *Atmosphere* **2023**, *14*, 372. https://doi.org/10.3390/atmos14020372

Academic Editors: Chong Wei, Chong Shi, Nan Li and Xingjun Xie

Received: 30 December 2022
Revised: 7 February 2023
Accepted: 11 February 2023
Published: 14 February 2023

1. Introduction

European Member States are committed to shift into a climate neutral economy by 2050 [1]. European Climate Law sets the intermediate target of reducing greenhouse gas (GHG) emissions by at least 55% by 2030 [2]. The transition to a neutral-climate continent requires the commitment and contribution of all sectors. In 2021, the EU Members emitted 3,641,710.673 kt CO_2 eq. [3]. The manufacturing and energy sectors were responsible for the most emissions, followed by transportation and agriculture [4].

According to IPCC methodology [5], GHG emissions from agriculture include: enteric fermentation (CH_4), manure management (CH_4, N_2O), agricultural soils (CO_2, CH_4 N_2O), field burning of agricultural residues (CH_4, N_2O), liming (CO_2) and urea application (CO_2). More than 80% of total agricultural GHG emissions are CH_4 emissions from enteric fermentation and N_2O emissions from soils in Europe [6]. Both those gases have much higher 100-year global warming potential (GWP-100) than carbon dioxide (CO_2), equal to 273, 27 and 29.8 for N_2O, CH_4-non fossil and CH_4-fossil, respectively [7]. Therefore, despite a relatively small share in total GHG emissions equal to ~13% [4], the agricultural

sector has great potential to reduce its emissions [8] since this sector is responsible for 53% of CH_4 emissions [9]. GHG emissions from agriculture are related to cultivation, variety of crops, rearing livestock and related equipment and can be categorized in three tiers of carbon footprinting: (1) energy input through machinery, electricity, livestock management and fossil fuels; (2) crop cultivation; (3) land use changes including conversion of natural ecosystems to agriculture and deforestation [10].

Poland is one of the main agricultural producers in the EU. In 2021, Poland harvested 34.0 million tonnes of cereals (11.4% of EU total) and was the third country after France (66.9 million tonnes; 22.5% of EU total) and Germany (42.4 million tonnes; 14.3% of EU total). The harvested rape and turnip rape seeds were equal to 3 million tonnes in 2021 and contributed 18% to the EU's total [11].

In Poland, cereal covers the highest crop area, followed by industrial crops and fodder crops. In cereal production, winter wheat is the main crop; in industrial crops, the oilseed rape has the highest share; and in fodder crops, maize dominates. Maize is an important fodder in Polish agriculture which is based on cereals and dairy cow production. Wheat covers ~30% of cereals area and contributes ~35% in cereal crops. Rape oilseed is the main raw material for edible oil produced in Poland. Maize and oilseed rape are also the main raw materials for biofuel production. Maize silage is one of the most important feedstocks for biogas production while oilseed rape is used for biodiesel production [12]. The GHG emissions from raw material production for fuel purposes may decide if biofuel can be considered sustainable and socially acceptable. In Poland, the average GHG emissions generated in the production of rapeseed for fuel equals to 24.28 g CO_2 eq. MJ^{-1} [13]. Maize cultivation generates 77.1 kg CO_2 eq. $t_{DM}{}^{-1}$ [14].

Carbon flux in both natural and cultivated ecosystems has seasonal variations closely related to plant growth [15,16]. The carbon fluxes in cropland are related to human activity such as agronomic measures, the planting pattern or in some regions, the irrigation system [17]. In the vegetation period, or more precisely between sowing and harvest, crops may serve as a carbon sink [16,18]. In pea and maize cropping systems, the CO_2 uptake offsets N_2O and CH_4 emissions [18]. The wheat, maize and wheat-maize cropping systems also behave as GHG sinks because of C sequestration [19]. Verma et al. [20] also reported that the rainfed maize–soybean rotation system is C neutral. If irrigation is used, the same rotation becomes a moderate C source, while continuously irrigated maize is nearly C neutral or a slight C source. Peng et al. [21], however, reported that maize cropping systems are a net carbon source if the carbon input with seeds and output at harvest are taken into account. The comparison of wheat and maize revealed that wheat is a weak C sink, while maize is close to CO_2 neutral to the atmosphere. However, when considering the total CO_2 loss in the fallow period, the full crop cultivation cycle of both crops were weak CO_2 sources [22]. The crop rotation is one of the most crucial factors affecting the C budget. Lehuger et al. [23] reported that wheat–maize–barley rotation was a net C source while oilseed rape–wheat–barley rotation was a net C sink due to higher C sequestration and C return from crops. Results given by Wen et al. [24] revealed that oilseed rape crops behave as C sinks and the sequestration potential rises with the growth stage in the following order: flowering stage, pod stage, bolting stage and seedling stage. The objective of this study was to determine the CO_2 exchange intensity in three different crops during the same growing season and identify the crop which is characterized by the highest reduction in CO_2 emission throughout the vegetation period. We hypothesize that: (1) there are differences in CO_2 fluxes in three different crops (summer maize, winter oilseed rape and winter wheat) and (2) the fluxes are influenced by crops and biomass growth.

2. Materials and Methods

2.1. Study Site

Three adjacent fields located 19 km south of Białystok, Poland (53°17′ N, 23°11′ E, 147 m a.s.l.) were chosen to conduct the CO_2 flux measurements. The study was conducted in similar microclimatic conditions on arable fields with most popular crops in Poland such

as summer maize (*Zea mays* L.), winter oilseed rape (*Brassica napus* L.) and winter wheat (*Triticum aestivum* L.). The field area of maize was 44 ha, the area of oilseed rape was 53.6 ha and the wheat field area was 11 ha. The study area has flat topography associated with Riss glaciation. The relief was softened by periglacial processes and transformed through fluvial processes [25]. The area is characterized by the temperate climate with continental influences, with an average annual temperature of 7.6 °C (for period of 1995–2019) and an average annual precipitation of 642 mm (for period 1995–2019), with peaks in July and August. The prevailing wind direction is west [26]. In all fields, the soil is classified as Luvisols [27]. In the maize and oilseed rape fields, the topsoil texture is loamy sand and in wheat field sandy loam dominates.

2.2. Experimental setup

The CO_2 fluxes (CO_2 exchange between plant canopy, soils and atmosphere) with other microclimatic conditions (air temperature (Ta), air relative humidity (RH), solar radiation (Rg), net radiation (Rn), photosynthetic photon flux density (PPFD), soil heat fluxes (SHF), soil water content (SWC), soil temperature (Ts), plant cover and plant height were determined on monthly or two week bases in all three fields in 3 measurement campaigns from spring 2016 to autumn 2016. The CO_2 fluxes in wheat field were measured on 8 test days: April 20, May 20, June 7, June 21, July 4, July 18, August 12, September 1. In oilseed rape field, the measurements were conducted on 10 test days: April 26, May 11, May 24, June 9, June 24, July 5, July 18, August 12, September 1 and September 14. In maize field, 7 test days were performed: May 13, May 19, June 6, June 14, June 28, July 25 and September 2. The dates of measurements were chosen so that no agrotechnical treatments were carried out at that time and, therefore, the emissions from fertilizers and fuel consumption were not taken into account in this study.

Soil physicochemical parameters were determined from samples taken in May (maize) and June (oilseed rape and wheat). Plant cover was measured using the digital photographs in squares of 1 m^2. We used a software program Corel PHOTO-PAINT^{TM} (CorelDRAW® Graphics Suite, Alludo, Ottawa, Canada) to divide the images into different ground cover classes based on the similarities among the pixels. The height of plants was measured with the meter stick in the field.

2.3. Soil Sampling and Analysis

Soil was sampled from the upper 20 cm of the soil profile. Five soil samples were taken with spatula from five sampling sites in each field. The sample from each sampling site was taken from five randomized points and mixed thoroughly. The samples were air-dried and sieved through a 2-mm mesh to separate the fine fraction and remove gravel. Roots were also removed before analytical analyses. Particle-size distribution was determined according to the hydrometer method [28]. Soil pH was measured in 1:2.5 soil/water suspension with HQ40D meter (Hach, Loveland, CO, USA). Soil organic carbon (SOC) content was determined with TOC-L analyser equipped with SSM-5000A solid sample combustion unit (Shimadzu, Kyoto, Japan) and total nitrogen (TN) content was measured with a Vapodest 50 s analyser (Gerhardt, Königswinter, Germany). After extraction with calcium lactate solution, the plant-available phosphorus (P_2O_5) was determined with the ammonium metavanadate method using UV-1800 spectrophotometer (Shimadzu, Kyoto, Japan), and the plant-available potassium (K_2O) was analysed using flame photometry (BWB Technology, Newbury, UK) [29].

2.4. Eddy Covariance Measurements

The fluxes in CO_2 were measured with eddy covariance (EC) system which consisted of LI-7500A (LI-COR Biosciences, Lincoln, NE, USA) open-path analyser to measure CO_2/H_2O concentrations and sonic anemometer WindMaster (Gill Instruments Limited, Lymington, UK) to measure three-dimensional wind speed, wind direction and sonic temperature. Measurements were conducted with a frequency of 10 Hz. Due to the fact

that this study aimed to directly compare variations in CO_2 flux in different crops during growing season, the EC system was moved among three studied crop fields (Figure 1). Each test day, EC system was installed in various parts of the currently studied crop field, depending on the wind direction, so that the results were obtained each time from the studied crop field. In order to have sufficient fetch which represents studied crop field, all sensors were fixed 200 cm above the ground or canopy layer. In the maize field, a geodetic stand was used to reach the required height. The measurements were conducted between 10:00 a.m. and 2:00 p.m. to minimize the diurnal variation in flux patterns since at this time of the day the wind conditions were the most stable in terms of speed and direction. Earlier in the morning, the wind speed was too low, while in the afternoon, wind direction was changing hampering the flux measurement from the studied field. The hourly interval was chosen based on the earlier observations of wind conditions. Nevertheless, the choice of measurement protocol with relatively short measurement period resulted in the lack of important information related to gas exchange. During all measurements, friction velocity (u*) was above 0.15 m s^{-1}.

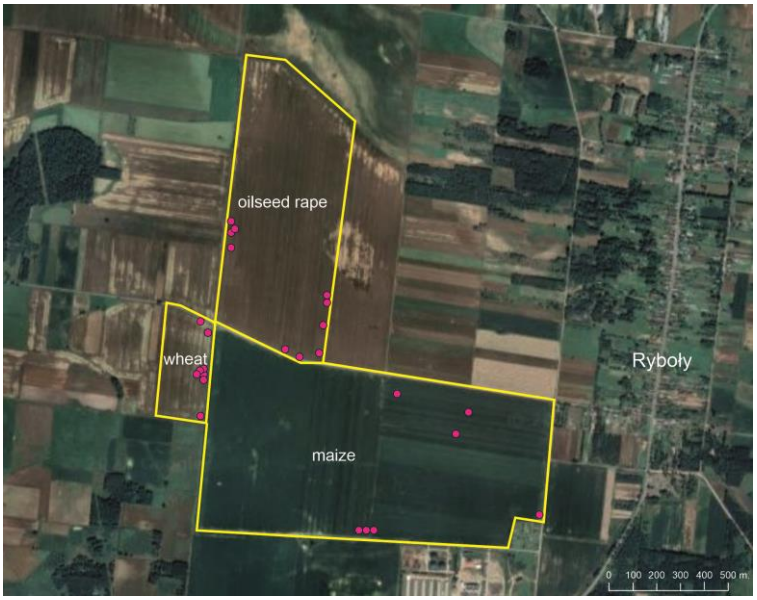

Figure 1. Location of eddy covariance tower (pink spots) on every test day on winter wheat, oilseed rape and maize fields.

Data logger Xlite 9210 (Sutron, Sterling, VA, USA) was used for recording the data from EC sensors. In order to refine the final CO_2 fluxes from the study fields, they were calculated for periods of 5 min using the EddyPro5 software package. The following calculation procedures were applied: spectral corrections [30,31]; compensation for density fluctuations [32]; sonic temperature correction for humidity [33]; time lag adjustment; coordinator rotation; block averaging; and statistical tests [34]. The footprint was estimated according to Kljun et al. [35]. Daily fluxes were calculated as extrapolation between measured values and weighted average for the vegetation period was calculated on the basis of daily CO_2 fluxes and days.

During flux measurements, microclimate of the currently studied field was analysed with the following set of sensors connected to the data logger: pyranometer sensor LI-200SL-50 (LI-COR, Lincoln, NE, USA), quantum sensor LI-190SL-50 (LI-COR, Lincoln, NE, USA), net radiometer NR Lite2, (Kipp&Zonen, Delft, The Netherlands), air temperature and relative humidity probe HMP155, (Vaisala OYJ, Vantaa, Finland), three soil heat flux plates HFP01 (Hukseflux Thermal Sensors B.V., Delft, The Netherlands), three soil temperature and water content sensors Hydra Probe II (Stevens Water Monitoring System Inc., Portland, OR, USA). Metrological data were recorded every 1 min. The sensors of soil temperature

and water content were inserted vertically into soil surface and heat plates were installed at depth of 5 cm.

2.5. Statistical Analyses

The significant differences in chemical properties amongst soils from all studied fields were assessed with one-way analysis of variance (ANOVA). Differences between means were determined using Tukey's test. The homogeneity of variance and normality was checked prior to ANOVA using the Brown–Forsythe and Shapiro–Wilk tests, respectively. When data failed the Shapiro–Wilk test, the F Welsh test was used for assessment of the significance of differences amongst the chemical properties. The Kruskal–Wallis test was performed when data failed the Brown–Forsythe test, indicating the inhomogeneity of variance. The significant differences amongst CO_2 fluxes were also analysed with the Kruskal–Wallis test. Spearman correlation coefficients were calculated for CO_2 fluxes and microclimatic variables to point out the main factors that influenced values of CO_2 fluxes. The level of accepted statistical significance was $p < 0.05$. All the statistical analyses of data were performed using STATISTICA 13.3 software (TIBCO Software Inc., Palo Alto, CA, USA).

3. Results

3.1. Soil Properties

In the maize and oilseed rape fields, the topsoil texture is loamy sand and in the wheat field, sandy loam dominates. The pH in all the soils indicated the slightly acidic conditions (Table 1). The SOC content was similar in the soil from the maize field and from the wheat field, even though these soils were characterized by different texture. The SOC concentration in the soil from oilseed rape was significantly ($p < 0.05$) lower. Contradictory, total N content was significantly higher ($p < 0.05$) in the soil from the wheat field compared to soils from the maize and oilseed rape fields. These differences resulted in a significantly ($p < 0.05$) higher C/N ratio in soil from the maize field. The plant-available phosphorus content followed the pattern of total N; however, its concentration in the soil from wheat was twofold lower than its content in the two other studied soils. In the soils from maize and oilseed rape, P_2O_5 concentration was remarkably high and in the soil from wheat, it was average, according to the Egnér–Riehm limit values [36]. The plant-available potassium concentration in all soils ranged from 17.3 ± 8.5 mg 100 g^{-1} to 22.3 ± 0.8 mg 100 g^{-1}. Since K_2O concentration in the two soils from the oilseed rape and the wheat fields were characterized by very high variability, there was no statistically detected differences amongst all studied soils. According to the Egnér–Riehm limit values [36], the average soil from the maize field was characterized by remarkably high K_2O content, the soil from the oilseed rape field had high K_2O concentration, while in the soil from the wheat field, average K_2O content was observed.

Table 1. Soil properties (means ± standard deviations) from wheat, maize and oilseed rape fields.

Crop	Soil Texture Soil Fraction (mm)			pH		SOC	N	C/N	P_2O_5	K_2O
	2–0.05	0.05–0.002	<0.002	H_2O	KCl					
Maize	79 ± 1 a	20 ± 1 a	1 ± 1 a	6.5 ± 0.4 a	5.6 ± 0.4 a	12.0 ± 0.4 a	1.0 ± 0.1 a	11.6 ± 0.4 a	28.7 ± 2.3 a	22.3 ± 0.8 a
Oilseed rape	74 ± 4 a	24 ± 3 a	2 ± 1 a	6.3 ± 0.2 a	5.4 ± 0.5 a	9.1 ± 1.8 b	0.9 ± 0.2 a	9.4 ± 0.5 b	29.7 ± 10.4 a	17.3 ± 8.5 a
Wheat	66 ± 3 b	30 ± 1 b	4 ± 2 b	6.5 ± 0.6 a	5.6 ± 0.9 a	13.8 ± 1.0 a	1.5 ± 0.2 b	9.1 ± 0.3 b	12.5 ± 4.3 b	18.0 ± 5.6 a

Soil texture—content of soil fractions (%), pH—reaction, SOC—soil organic carbon (g kg^{-1}), N—total nitrogen (g kg^{-1}), P_2O_5—plant-available phosphorus (mg 100 g^{-1}), K_2O—plant-available potassium (mg 100 g^{-1}). Lowercase letters—statistical differences at $p < 0.05$.

3.2. Meteorological and Soil Conditions

The meteorological conditions prevailing in the study area during the measurements were relatively even (Table 2). Ta was ~20 °C for most of the study period, while RH was ~50%. In most measurement days, PPFD exceeded the value of 1000 μmol m^{-2} s^{-1}, fostering the process of photosynthesis. The maximum value of 1740.68 μmol m^{-2} s^{-1} was reached during measurements over the oilseed rape field. Values lower than 1000 μmol m^{-2} s^{-1} were observed only on three measurement days.

Table 2. Microclimatic conditions during measurements in the studied fields.

Date	Ta	RH	Rg	Rn	PPFD	SWC	Ts
			Wheat field				
April 20	9.64	49.69	552.79	313.70	1133.70	0.17	14.83
May 20	17.49	50.00	683.15	443.54	1369.88	0.20	22.69
June 7	16.04	39.74	830.96	547.33	1666.39	0.17	24.07
June 21	18.96	74.83	587.12	425.87	1221.42	0.17	22.81
July 4	19.48	53.25	567.84	376.98	1162.47	0.20	21.63
July 18	20.36	55.84	559.99	433.82	1220.34	0.23	23.58
August 12	17.61	47.44	651.69	408.85	1308.96	0.26	16.36
September 1	20.51	54.32	529.41	267.87	1076.29	0.10	25.21
			Oilseed rape field				
April 26	7.51	58.36	459.62	246.06	931.03	0.07	11.60
May 11	21.07	48.60	597.37	358.03	1129.51	0.05	20.98
May 24	22.59	38.06	846.81	528.68	1740.68	0.06	20.66
June 9	15.92	49.67	766.30	496.95	1564.39	0.07	20.52
June 24	27.76	53.25	777.71	555.45	1631.78	0.05	25.96
July 05	21.50	45.58	726.03	511.83	1284.06	0.08	24.48
July 18	18.65	61.79	399.62	281.93	768.36	0.18	19.85
August 12	18.21	43.79	531.09	290.68	1055.89	0.15	23.39
September 1	21.65	52.65	571.11	330.57	1212.29	0.05	27.98
September 14	19.86	50.59	632.60	327.22	1355.50	0.03	26.46
			Maize field				
May 13	20.64	49.87	535.68	304.11	1126.53	0.09	26.29
May 19	15.40	29.47	398.19	214.14	808.27	0.13	20.40
June 3	22.65	43.70	799.48	498.77	1629.50	0.14	30.03
June 14	20.57	44.93	568.70	327.36	1164.00	0.04	25.92
June 28	20.67	55.36	524.84	330.34	1076.65	0.02	28.83
July 25	26.50	60.25	779.95	529.63	1554.20	0.04	35.79
September 2	21.79	55.43	662.98	328.18	1338.19	0.02	27.07

Ta—air temperature (°C), RH—air relative humidity (%), Rg—solar radiation (W m^{-2}), Rn—net radiation (W m^{-2}), PPFD—photosynthetic photon flux density (μmol m^{-2} s^{-1}), SWC—soil water content (m^3 m^{-3}), Ts—soil temperature (°C).

In all studied fields, Ts was similar. The only difference among the studied soils was observed for the SWC which was higher in the wheat field, characterized by slightly finer material of sandy loam, compared to loamy sand in the maize and oilseed rape fields.

3.3. Vegetation Development

In the wheat field, the measurements started on April 20 in the wheat tillering phase, when plants with a height of ~10 cm covered ~10% of the field (Figure 2). In the tillering stage, the wheat growth was relatively slow, since within a month, plants reached 35 cm and covered about 40% of the field and entered the stem elongation stage. In the next two weeks, the wheat growth rate accelerated and plants with a height of 80 cm covered ~80% of the field. In the flowering stage, both the height and the degree of coverage of the field by vegetation changed only slightly. Wheat reached the development of fruit stage at the

beginning of August and entered the senescence stage in the second half of July. The height of the plants and cover was stable in this period until the harvest on August 20.

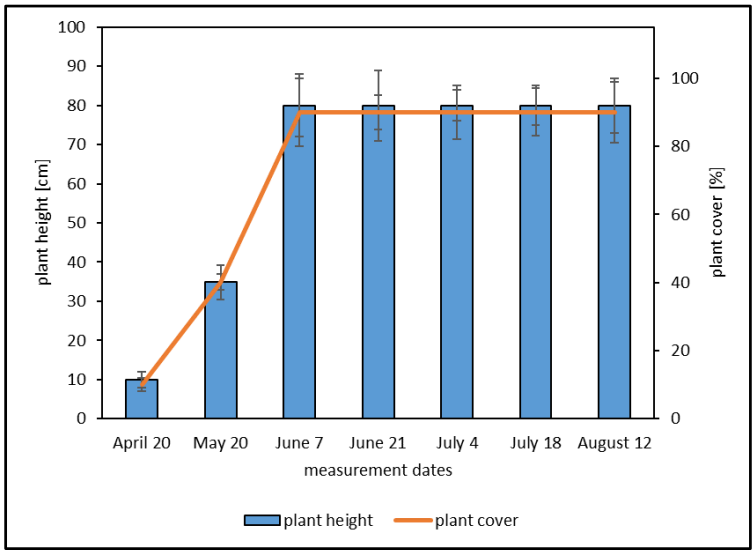

Figure 2. Vegetation development in the wheat field.

The field measurement in the oilseed rape started on April 26 when plants were already ~40 cm high and covered ~25% of the field (Figure 3). In the next two weeks, the plants grew to 90 cm in height and almost completely covered the field. At the end of this period, plants started the flowering stage which lasted altogether four weeks. In the flowering stage, the crop is in full flower which means that 50% of flowers on the main raceme are open. This is accompanied by yellow colour in the crop field. On June 9, plants were in the fruit development stage, when elongated green pods develop from pollinated oilseed rape flowers. The next measurement on June 24 was performed on the plants in the seeds ripening stage, in which pods at first are soft and green and in next 10 days they turn brown. At the senescence stage, seeds became hard and black and the plants were harvested at the end of July. Oilseed rape was followed by charlock sown for green manure. Initially, charlock covered a small area of the field, but after reaching a height of ~25 cm, almost the entire field was covered with a green cover.

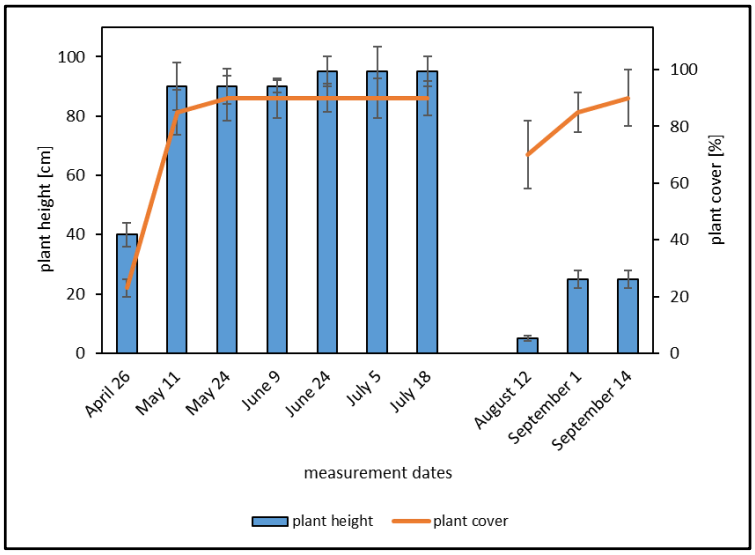

Figure 3. Vegetation development in the oilseed rape field.

In the maize field, the first measurement was conducted on May 13, just after the emergence stage. In the first leaf collar stage, plants were 6 cm high and covered about 1% of the area (Figure 4). The maize was sown at an average of 12 plants per m^2. A week later, the plants in the second leaf collar stage were ~10 cm high and covered 3% of the field. In the next two weeks, the plants grew faster, reaching a height of 40 cm and covering 30% of the field, entering the stem elongation stage. In this stage, in the next 10 days, the maize grew to 80 cm and covered about 50% of the area. During the following two weeks, still in stem elongation stage, plants reached a height of 140 cm and covered ~70% of the field. From that moment, the plant cover increased very slowly, even though the maize was still growing. On the next measurement day (July 25), the plants reached 220 cm and were in the flowering stage. For the next month, the plant cover was rather stable. The maize was harvested on September 7 at the end of the fruit development stage and ploughing took place the next day. The field was left fallow for winter.

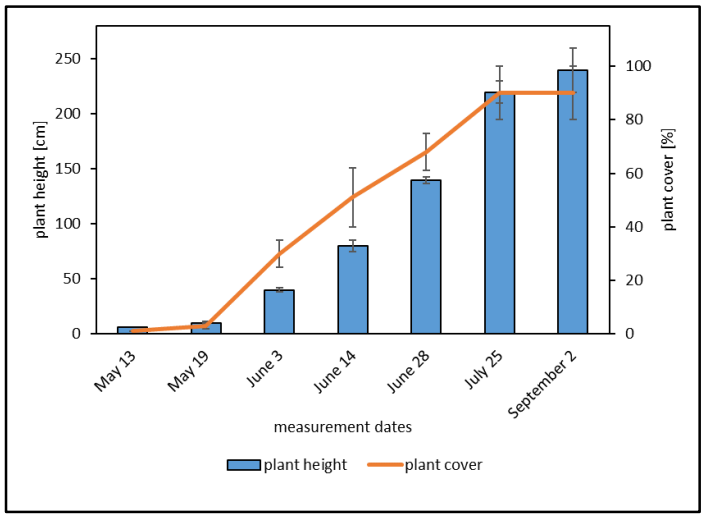

Figure 4. Vegetation development in the maize field.

3.4. CO_2 Fluxes

The seasonal dynamics of CO_2 fluxes in winter wheat and oilseed rape were similar but differed significantly ($p < 0.05$) from maize due to the individual dynamics in atmospheric CO_2 assimilation of each species through the growing season (Figure 5). The CO_2 absorption capacity is related to the vegetation development stage since changes in biomass and the level of chlorophyll in plants affects the photosynthesis process.

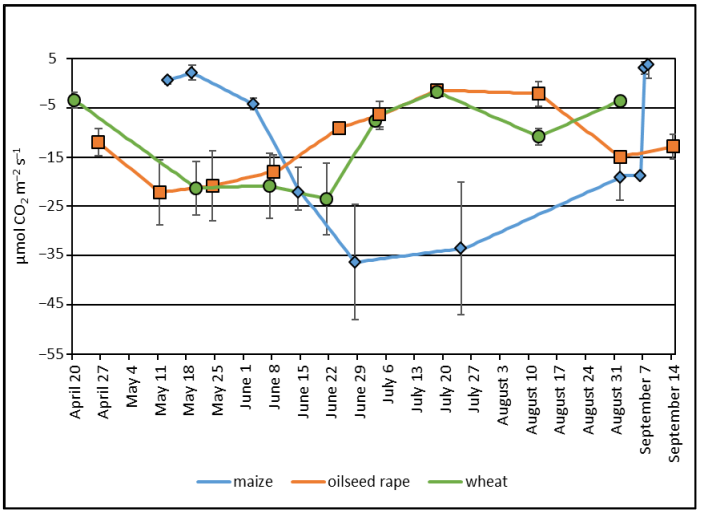

Figure 5. The CO_2 fluxes in wheat, oilseed rape and maize fields.

During the tillering stage of wheat growth, despite the slight enlargement in biomass, the CO_2 flux increased to over -20 µmol CO_2 m^{-2} s^{-1} and remained on this level till the end of June. Thus, during the fast-growth stage of stem elongation, the photosynthesis exceeded the respiration. In the next stages, from flowering to senescence, the significant drop in the CO_2 absorption from the atmosphere was observed related to the decrease in chlorophyll levels indicated by colour change in the plants (Figure S1). Nevertheless, the CO_2 flux was negative, indicating that the respiration was lower than photosynthesis for all the growing season.

Similar seasonal dynamics in CO_2 fluxes were observed for oilseed rape; however, from April to mid-May, the CO_2 flux slightly exceeded the values measured for wheat. The negative values indicate that photosynthesis in the inflorescence emergence stage was higher than respiration. The constant drop in CO_2 fluxes was observed from May 11, indicating that in the next growth stages, beginning from the flowering stage through to the fruit development and ripening stages, carbon capacity of the oilseed rape field was getting weaker (Figure S2). The lowest value of -1.7 µmol CO_2 m^{-2} s^{-1} was reached on July 18 in the senescence stage. The increase in CO_2 absorption in August was related to the growth of charlock as a cover crop in the field after the oilseed rape was harvested at the end of July.

Contrary to the wheat and oilseed rape, CO_2 assimilation by the maize field was the most intensive in the second half of the vegetation period, when plants were finishing the stem elongation stage (Figure S3). In the first month of the study, when the plant cover was less than 30% of the field and the plants were ~30 cm high (Figure S3), CO_2 absorption reached a value similar to that of the wheat and oilseed rape fields. A further increase in maize biomass in the next two weeks resulted in the CO_2 flux of more than -35 µmol CO_2 m^{-2} s^{-1}, indicating rising carbon absorption of the maize field during this time. The CO_2 flux remained at a similar level for the next two weeks, indicating that the photosynthesis was much stronger than respiration. During the next 6 weeks, due to a gradual decrease in the intensity of photosynthesis, the CO_2 flux dropped to about -20 µmol CO_2 m^{-2} s^{-1}.

The weighted average values of CO_2 fluxes calculated for the entire vegetation period were -22.22 µmol CO_2 m^{-2} s^{-1}, -14.27 µmol CO_2 m^{-2} s^{-1} and -11.95 µmol CO_2 m^{-2} s^{-1} for maize, oilseed rape and wheat, respectively. Conversion of these values into the amount of assimilated carbon revealed the following results: -160 g CO_2-C ha^{-1} min^{-1}, -102 g CO_2-C ha^{-1} min^{-1} and -86 g CO_2-C ha^{-1} min^{-1} for maize, oilseed rape and wheat, respectively.

The field cultivation after harvest affected the annual CO_2 fluxes. The wheat and oilseed rape were harvested at the end of August while maize was mown in late August and early September. Leaving the maize field after harvest uncovered with any crop (Figure S4) resulted in positive values of CO_2 flux, indicating the loss of CO_2 assimilation and the start of CO_2 emissions. In the wheat field, after harvest, the CO_2 fluxes were still negative, indicating the higher CO_2 absorption over respiration. Indeed, weeds covered the soil below the wheat canopy in the senescence stage and after the crop harvest; they continued to support photosynthesis. The oilseed rape harvest was followed by charlock as a cover crop. The rapid growth of charlock resulted in the development of almost complete plant cover in the field and negative values of CO_2 fluxes, indicating growing carbon absorption capacity of the oilseed rape field after harvest.

In the wheat field, CO_2 fluxes were significantly ($p < 0.05$) correlated with PPFD, Rg and Rn as well as with Ts (Table 3). In the case of oilseed rape, correlations with all analysed parameters were significant ($p < 0.05$), with CO_2 fluxes positively correlated with SWC and Ts. In the maize field, the relationship between CO_2 fluxes was significant ($p < 0.05$) with Ta, RH, Rn, SWC and Ts, but was only positive for SWC.

Table 3. Correlation between CO_2 fluxes and microclimatic conditions in the studied fields.

	CO_2 Flux	Ta	RH	Rg	Rn	PPFD	SWC	Ts
Wheat field								
CO_2 flux	1	−0.03	−0.11	**−0.46**	**−0.47**	**−0.44**	−0.01	**−0.47**
Ta		1	**0.49**	0.11	**0.27**	0.14	**0.35**	**0.53**
RH			1	**−0.24**	−0.14	**−0.22**	−0.13	0.06
Rg				1	**0.97**	**0.99**	**0.18**	**0.30**
Rn					1	**0.98**	**0.21**	**0.41**
PPFD						1	**0.17**	**0.32**
SWC							1	**0.32**
Ts								1
Oilseed rape field								
CO_2 flux	1	**−0.14**	**0.21**	**−0.33**	**−0.26**	**−0.38**	**0.62**	**0.15**
Ta		1	**−0.46**	**0.45**	**0.48**	**0.39**	**−0.37**	**0.56**
RH			1	**−0.58**	**−0.52**	**−0.51**	0.05	**−0.31**
Rg				1	**0.96**	**0.91**	**−0.12**	**0.29**
Rn					1	**0.87**	−0.04	**0.28**
PPFD						1	**−0.21**	**0.26**
SWC							1	**−0.37**
Ts								1
Maize field								
CO_2 flux	1	**−0.20**	**−0.14**	−0.07	**−0.21**	−0.04	**0.44**	**−0.38**
Ta		1	−0.05	**0.56**	**0.57**	**0.58**	**−0.14**	**0.86**
RH			1	−0.02	−0.06	−0.05	**−0.50**	0.02
Rg				1	**0.92**	**0.96**	**0.16**	**0.54**
Rn					1	**0.86**	**0.17**	**0.59**
PPFD						1	**0.14**	**0.56**
SWC							1	**−0.17**
Ts								1

Ta—air temperature (°C), RH—air relative humidity (%), Rg—solar radiation (W m^{-2}), Rn—net radiation (W m^{-2}), PPFD—photosynthetic photon flux density (µmol m^{-2} s^{-1}), SWC—soil water content (m^3 m^{-3}), Ts—soil temperature (°C). Bold values show significant correlations ($p < 0.05$).

4. Discussion

4.1. Soil Properties and Plant Growth

Maize can be cultivated over wide climatic and soil conditions; however, warm frost-free weather with high insolation is essential for high yields [37]. Maize is a rainfed crop but requires high soil moisture, even though it is a water-saving crop, and its transpiration rate is lower than that of other cereals and forage crops. Maize can be grown over a wide range of soils but performs best on well-structured, fertile soils containing high amounts of organic matter and plant-available nutrients [38,39]. Soils suitable for maize cultivation should offer proper aeration and drainage and at the same time should maintain enough water [38]. Heavy and cold soils which are poorly drained or dry sandy and too acidic soils are not suitable for maize cultivation [39]. The optimum pH for maize is between 5.8 and 6.8, but this crop also may be highly productive on slightly acidic soils with a pH of 5.5 [37,40]. In this study, the soil from the maize field was characterized by pH of 6.5 (Table 1), which is an optimum range for maize growth. The content of plant-available P and K was also remarkably high in the studied soil (Table 1) and resulted in a high growth rate in the maize [41,42]. Potassium is one of the essential nutrients for crop growth and yield, although it is not a component of tissues but is associated or involved in many physiological processes such as photosynthesis, assimilate transport, water relations and protein metabolism which support the growth of plants [43,44]. A higher K content in soil and an optimal K fertilization improve soil fertility and support the high grain yield [45].

Winter wheat is highly resistant to low temperatures during the early stages of plant development and near freezing temperatures in this growth phase are required for vernalization [46]. Wheat is grown as a rainfed crop; however, this plant requires relatively high soil moisture, especially for germination and several growth stages in autumn and spring. The adequate amount of stored water is particularly important due to a less developed root system. Excessive rainfalls, especially in the period from earing to the end of ripening are also unfavourable [47,48]. Growth is then prolonged, and plants can be easily affected by diseases [47]. Wheat has the highest soil requirements of all cereals mainly due to a less developed root system and, therefore, a lower ability to take up nutrients. Wheat grows best on well-drained, well-structured soils with high water capacity [48]. A soil pH between 6.0 and 7.0 is optimal for micronutrient availability and wheat growth. The most limiting factor is the N content in soil. Its deficiency leads to lower crops while its excess increases plant susceptibility to diseases, lodging and spring freeze damage [49]. In this study, the soil from the wheat field was characterized by a pH of 6.5 (Table 1), which is in the optimum range for wheat growth. Sandy loams with a high SOC and N content and a remarkably high content of plant-available P and K (Table 1) were favourable for wheat cultivation. A higher content of clay and silt compared to loamy sands from the maize and oilseed rape fields might increase the water capacity and, thus, create good water conditions for wheat growth reflected by a higher SWC on all test days (Table 2).

Oilseed rape grows best in a temperate climate and during its lifecycle it can be exposed to extreme temperatures; however, in the flowering stage it is very susceptible to even short periods of drought. Water stress decreases the leaf area index (LAI), nitrogen nutrition index and leaf chlorophyll [50]. Oilseed rape has remarkably high nutritional and water requirements. The crop grows best on deep, medium-textured, well-drained, humus and calcium-rich soils [51] with an optimum pH at 5.7–7.0. Sandy, poor, acidic and dry soils, or heavy, waterlogged soils are unsuitable for oilseed rape cultivation [51]. In this study, the soil from the oilseed rape field was characterized by pH 6.3, which was in the optimum range. The content of plant-available P and K was remarkably high and despite the low SOC content, the C/N ratio was narrow, which indicates a rapid rate of organic matter transformation.

4.2. CO_2 Fluxes

4.2.1. CO_2 Fluxes from Agro-Ecosystems

Various ecosystems, including agricultural land, can act both as a sink and as a source of carbon [52], and even slight changes during growing season can result in annual changes in CO_2 flux. The net ecosystem exchange of CO_2 refers to the difference between the carbon fixation in photosynthesis and its release because of ecosystem respiration [53]. The net vertical CO_2 flux has a specific value and return. Negative net flux indicates the CO_2 transport downwards to the active surface, i.e., the predominance of absorption processes over emission. In turn, a positive net flux indicates the upward transport from the active surface to the atmosphere, i.e., the predominance of emissions over absorption. Soil cultivation is another source of significant GHG emissions including emissions from the use of mineral fertilizers and fuel and emissions from soil, which are the main sources of CO_2 and N_2O. However, proper agronomic practices often supply the soil with organic matter and reduce the intensity of its decomposition and, thus, increase the carbon stock in the soil [54]. In this study, the CO_2 fluxes (CO_2 exchange between plant canopy, soils and atmosphere) were measured on days in which the agrotechnical practices were not performed, therefore the CO_2 emissions from them were not included. This allowed us to focus only on CO_2 emissions and the absorption of the studied agro-ecosystems and recognize them as a C sink during the growing period.

4.2.2. Effect of Plant Development Stages on CO_2 Fluxes

CO_2 emissions from agricultural land can be offset through the binding of this compound with the growing vegetation through photosynthesis. However, the efficiency of this process depends to a considerable extent on the rate of vegetation development as well as on the land use. According to the research of Xu and Baldocchi [55], seasonal trends in carbon fluxes in agro-ecosystems follow closely the change in the development of plant cover, which is the result of the phenological phases of plants. In the studies of Jans et al. [56], maximum daily CO_2 fluxes in a corn field were associated with a peak growth period. A strong relationship between CO_2 fluxes and the size of the plant cover expressed by the LAI was also shown by Wang et al. [57]. Liu et al. [53] also reported a rapid increase in CO_2 flux in the fields covered by winter oilseed rape when the plants turned green, with its maximum at the jointing-booting and heading-filling stages, and a gradual decrease at the milk ripening-maturity stage. These changes resulted from lower LAI, chlorophyll and enzyme content during the early growth stage of wheat, which determined a relatively low photosynthetic efficiency of plants. LAI, chlorophyll content and enzymatic activity reached their maximum with wheat growing stages; thus, the plants were capable of relatively high photosynthesis during the flowering phase. In the later part of the growing season, both enzyme activity and chlorophyll content decreased due to the aging of the leaves, which resulted in a decrease in the intensity of photosynthesis.

In this study, both wheat and oilseed rape relatively quickly fully covered the field, which resulted in the whole area of the field participating in the photosynthesis process. At the same time, sparsely planted maize left a significant area of the field uncovered with leaves. In mid-June, CO_2 assimilation by maize rapidly increased, while in the case of the wheat and oilseed rape, the CO_2 absorption decreased as a result of entering the stage of flowering and developing of fruits which in both plants was manifested by the loss of the chlorophyll responsible for photosynthesis. In the same period, maize growing gradually covered the entire field, which resulted in the maximum intensity of CO_2 assimilation which started at the end of June in the stem elongation stage and lasted on a stable level through the flowering stage until the development of fruit stage at the end of August.

4.2.3. CO_2 Flux Values in Winter Wheat, Oilseed Rape and Maize Fields

Liu et al. [53] reported CO_2 flux values in winter wheat field ranging from -1738 mg CO_2 m^{-2} h^{-1} to -541 mg CO_2 m^{-2} h^{-1} in two studied growing seasons. In our study, this range was much wider from -3721 mg CO_2 m^{-2} h^{-1} to -537 mg CO_2 m^{-2} h^{-1}. Despite this difference, the relationships between CO_2 assimilation and vegetation development found in the analysed agro-ecosystems were similar. Eshonkulov [58] reported -198 g CO_2-C ha^{-1} min^{-1} for a wheat field. This value is higher than that observed in this study (-169 g CO_2-C ha^{-1} min^{-1}). In this study, in the oilseed rape field, the maximum value of the CO_2 flux was observed on May 11 when it reached the value of -158 g CO_2-C ha^{-1} min^{-1}. This value is slightly higher than that reported by Eshonkulov [58], who also observed a value of -142 g CO_2-C ha^{-1} min^{-1} for an oilseed rape field in May. In the maize field, several months shift in the maximum CO_2 flux compared to the wheat field and the oilseed rape fieldwhich was observed in this study, is in a good agreement with the results revealed by Eshonkulov [58] who reported a maximum flux in August equal to -211 g CO_2-C ha^{-1} min^{-1}, which is a much lower value compared to the result of this study (-262 g CO_2-C ha^{-1} min^{-1}). The fluxes observed in the maize field in this study are higher than the values presented by Zhang et al. [59], who studied the daily distribution of CO_2 exchange over various ecosystems and reported a maximum value for maize equal to -193 g CO_2-C ha^{-1} min^{-1}.

4.2.4. Effect of Microclimatic Variables on CO_2 Fluxes

CO_2 exchange between terrestrial ecosystems and the atmosphere depends to a large extent on environmental variables [60]. Liu et al. [53] found that CO_2 fluxes are significantly correlated with PPFD, Ta, Ts, RH and SWC. Solar radiation is crucial for the photosynthesis process, therefore, among the factors listed above, PPFD is particularly important for the daily course of CO_2 flux. In this study, the value of this parameter remained at a high level, which was conducive to gas exchange. This process was also supported by other parameters measured in this study, i.e., solar radiation (Rg) and net radiation (Rn). The lack of a significant relationship between CO_2 fluxes and PPFD in the maize field was related to the low impact of this radiation on the absorption of CO_2 by poorly developed plants that covered a small area of the field. An equally positive effect on the process studied in this work was the relatively high Ta and Ts, which are the predominant limiting factors for the growth of plants and activity of the microbial community [57]. The SWC found in this study was conducive to CO_2 fluxes in all the studied fields. According to the research of Wang et al. [57], SWC higher than 0.25 m^3 m^{-3} may reduce gas exchange. This is because higher SWC reduces the water absorption rate of the root system leading to a decrease in the photosynthesis rate. A significant negative linear relationship between SWC and CO_2 flux during the post-milk ripening period in winter wheat fields was demonstrated by Liu et al. [53]. The positive correlation of CO_2 fluxes and SWC in oilseed rape and maize fields found in this study is the result of low water content in the soil, which in such amounts favours the development of plants, while not inhibiting the gas exchange process.

5. Conclusions

In this study, the CO_2 fluxes in summer maize, winter oilseed rape and winter wheat fields were measured using the eddy covariance system. The measurements were conducted from the early stage of plant development to the post-harvest period. This study revealed a large difference between maize and two other studied crops in terms of CO_2 exchange between the land surface and the atmosphere. Even though all the studied agroecosystems were carbon sinks, the intensity of carbon assimilation varied in individual fields during the study period. The highest negative values of CO_2 fluxes, indicating strong absorption of this gas in the photosynthesis process, were observed in the maize field due to the high production of maize biomass. However, the maize field was a carbon source for the greater part of the year due to slow growth of the plants at the beginning of the growing season, and due to leaving the field fallow after harvest until the next sowing. CO_2 exchange in wheat and oilseed rape fields was less intense, but more even throughout the growing season. In addition, the catch crop in the oilseed rape field contributed to the intensive absorption of CO_2 after harvesting the main crop. The differences in CO_2 fluxes between fields resulted from the plants' physiology and agrotechnical treatments; but, due to these features, the total amounts of carbon absorbed by the analysed crops are more even than the maximum CO_2 fluxes would indicate.

Supplementary Materials: The following are available online at https://www.mdpi.com/article/10.3390/atmos14020372/s1. Figure S1. The development stages of wheat on: 20 April 2016 (a), 20 May 2016 (b), 21 June 2016 (c), 18 July 2016 (d); Figure S2. The development stages of oilseed rape on: 26 April 2016 (a), 11 May 2016 (b), 9 June 2016 (c), 5 July 2016 (d); Figure S3. The development stages of maize on: 19 May 2016 (a), 14 June 2016 (b), 28 June 2016 (c), 2 September 2016 (d); Figure S4. The surface of the studied fields after harvest: a—wheat field, b—oilseed rape field, c—maize field.

Author Contributions: Conceptualization, R.C.; methodology, R.C.; validation, R.C.; formal analysis, R.C. and A.W.-C.; investigation, R.C.; writing—original draft preparation, R.C.; writing—review and editing, A.W.-C.; visualization, R.C. and A.W.-C. All authors have read and agreed to the published version of the manuscript.

Funding: The research was carried out as part of project No. WZ/WB-IIŚ/1/2020 at the Białystok University of Technology and financed from the research subsidy provided by the Minister of Education and Science.

Institutional Review Board Statement: Not applicable.

Informed Consent Statement: Not applicable.

Data Availability Statement: Not applicable.

Conflicts of Interest: The authors declare no conflict of interest. The funders had no role in the design of the study; in the collection, analyses, or interpretation of data; in the writing of the manuscript; or in the decision to publish the results.

References

1. European Commission. *The European Green Deal. Communication from the Commission to the European Parliament, the European Council, the Council, the European Economic and Social Committee and the Committee of the Regions*; COM (2019) 640 Final; European Commission: Brussels, Belgium, 2019.
2. Regulation (EU) 2021/1119 of the European Parliament and of the Council of 30 June 2021 Establishing the Framework for Achieving Climate Neutrality and Amending Regulations (EC) No 401/2009 and (EU) 2018/1999 ('European Climate Law'). *Off. J. Eur. Union* **2021**, *L 241*, 1–17.
3. European Environment Agency. GHG_proxy_2021. Available online: https://www.eea.europa.eu/data-and-maps/data/approximated-estimates-for-greenhouse-gas-emissions-5/2017-ghg-proxies/ghg_proxy_2017 (accessed on 29 November 2022).
4. Eurostat. File:Quarterly GHG Figures for Q2 2022 with GDP Ver2.Xlsx. Available online: https://ec.europa.eu/eurostat/statistics-explained/index.php?title=File:Quarterly_GHG_Figures_for_Q2_2022_with_GDP_ver2.xlsx (accessed on 29 November 2022).
5. Buendia, E.C.; Tanabe, K.; Kranjc, A.; Jamsranjav, B.; Fukuda, M.; Ngarize, S.; Osako, A.; Pyrozhenko, Y.; Shermanau, P.; Federici, S. *2019 Refinement to the 2006 IPCC Guidelines for National Greenhouse Gas Inventories*, 1st ed.; IPCC: Geneva, Switzerland, 2019.
6. European Environment Agency. National Emissions Reported to the UNFCCC and to the EU Greenhouse Gas Monitoring Mechanism. Available online: https://www.eea.europa.eu/ims/greenhouse-gas-emissions-from-agriculture (accessed on 30 November 2022).
7. IPCC. *Climate Change 2021: The Physical Science Basis*, 1st ed.; Contribution of Working Group I to the Sixth Assessment Report of the Intergovernmental Panel on Climate Change; Cambridge University Press: Cambridge, UK; New York, NY, USA, 2021.
8. Mielcarek-Bocheńska, P.; Rzeźnik, W. Greenhouse Gas Emissions from Agriculture in EU Countries—State and Perspectives. *Atmosphere* **2021**, *12*, 1396. [CrossRef]
9. van der Veen, R.; de Vries, M.; van de Pol, J.; van Santen, W.; Sinke, P.; de Vries, J.; Kampman, B.; Bergsma, G. *Methane Reduction Potential in the EU between 2020 and 2030*, 1st ed.; CE Delft: Delft, The Netherlands, 2022.
10. Jaiswal, B.; Agrawal, M. Carbon Footprints of Agriculture Sector. In *Carbon Footprints*; Muthu, S.S., Ed.; Environmental Footprints and Eco-design of Products and Processes; Springer: Singapore, 2020; pp. 81–99. ISBN 9789811379154.
11. Eurostat. Agricultural Production–Crops. Available online: https://ec.europa.eu/eurostat/statistics-explained/index.php?title=Agricultural_production_-_crops (accessed on 5 December 2022).
12. Statistics Poland. Production of Agricultural and Horticultural Crops. Available online: https://stat.gov.pl/obszary-tematyczne/rolnictwo-lesnictwo/uprawy-rolne-i-ogrodnicze/produkcja-upraw-rolnych-i-ogrodniczych-w-2021-roku,9,20.html (accessed on 3 December 2022).
13. Borzęcka-Walker, M.; Faber, A.; Jarosz, Z.; Syp, A.; Pudełko, R. Greenhouse Gas Emissions from Rape Seed Cultivation for FAME Production in Poland. *J. Food Agric. Environ.* **2013**, *11*, 1064–1068.
14. Wiśniewski, P.; Kistowski, M. Greenhouse Gas Emissions from Cultivation of Plants Used for Biofuel Production in Poland. *Atmosphere* **2020**, *11*, 394. [CrossRef]
15. Li, H.; Zhang, F.; Li, Y.; Wang, J.; Zhang, L.; Zhao, L.; Cao, G.; Zhao, X.; Du, M. Seasonal and Inter-Annual Variations in CO2 Fluxes over 10 Years in an Alpine Shrubland on the Qinghai-Tibetan Plateau, China. *Agric. For. Meteorol.* **2016**, *228–229*, 95–103. [CrossRef]
16. Schmidt, M.; Reichenau, T.G.; Fiener, P.; Schneider, K. The Carbon Budget of a Winter Wheat Field: An Eddy Covariance Analysis of Seasonal and Inter-Annual Variability. *Agric. For. Meteorol.* **2012**, *165*, 114–126. [CrossRef]
17. Guo, H.; Li, S.; Wong, F.-L.; Qin, S.; Wang, Y.; Yang, D.; Lam, H.-M. Drivers of Carbon Flux in Drip Irrigation Maize Fields in Northwest China. *Carbon Balance Manag.* **2021**, *16*, 12. [CrossRef] [PubMed]
18. Maier, R.; Hörtnagl, L.; Buchmann, N. Greenhouse Gas Fluxes (CO_2, N_2O and CH_4) of Pea and Maize during Two Cropping Seasons: Drivers, Budgets, and Emission Factors for Nitrous Oxide. *Sci. Total Environ.* **2022**, *849*, 157541. [CrossRef]
19. Tao, F.; Li, Y.; Chen, Y.; Yin, L.; Zhang, S. Daily, Seasonal and Inter-Annual Variations in CO_2 Fluxes and Carbon Budget in a Winter-Wheat and Summer-Maize Rotation System in the North China Plain. *Agric. For. Meteorol.* **2022**, *324*, 109098. [CrossRef]
20. Verma, S.B.; Dobermann, A.; Cassman, K.G.; Walters, D.T.; Knops, J.M.; Arkebauer, T.J.; Suyker, A.E.; Burba, G.G.; Amos, B.; Yang, H.; et al. Annual Carbon Dioxide Exchange in Irrigated and Rainfed Maize-Based Agroecosystems. *Agric. For. Meteorol.* **2005**, *131*, 77–96. [CrossRef]
21. Peng, X.; Ma, J.; Cai, H.; Wang, Y. Carbon Balance and Controlling Factors in a Summer Maize Agroecosystem in the Guanzhong Plain, China. *J. Sci. Food Agric.* **2023**, *103*, 1761–1774. [CrossRef] [PubMed]

22. Zhang, Q.; Lei, H.; Yang, D.; Xiong, L.; Liu, P.; Fang, B. Decadal Variation in CO_2 Fluxes and Its Budget in a Wheat and Maize Rotation Cropland over the North China Plain. *Biogeosciences* **2020**, *17*, 2245–2262. [CrossRef]
23. Lehuger, S.; Gabrielle, B.; Larmanou, E.; Laville, P.; Cellier, P.; Loubet, B. Predicting the Global Warming Potential of Agro-Ecosystems. *Biogeosciences Discuss.* **2007**, *4*, 1059–1092. [CrossRef]
24. Wen, S.; Gao, Q.; Gao, Z.; Lu, J. Variation Characteristics of Carbon Flux during the Whole Growth Period of Winter Rapeseed in Central Hunan Province. *Chin. J. Oil Crop Sci.* **2022**, *44*, 581–588. [CrossRef]
25. Richling, A.; Solon, J.; Macias, A.; Balon, J.; Borzyszkowski, J.; Kistowski, M. *Regional Physical Geography of Poland*, 1st ed.; Bogucki Wyd. Naukowe: Poznań, Poland, 2021. (In Polish)
26. Górniak, A. *Climate of the Podlaskie Voivodeship in the Time of Global Warming*, 1st ed.; Wydawnictwo Uniwersytetu w Białymstoku: Białystok, Poland, 2021. (In Polish)
27. IUSS Working Group WRB World Reference Base for Soil Resources 2014. *Update 2015 International Soil Classification System for Naming Soils and Creating Legends for Soil Maps*; FAO: Tome, Italy, 2015.
28. *PN-R-04032:1998*; Soil Sample Collecting and Analysis of Soil Texture. Polski Komitet Normalizacyjny: Warsaw, Poland, 1998. (In Polish)
29. Ostrowska, A.; Gawliński, S.; Szczubiałka, Z. *Methods of Analysis and Evaluation of Soil and Plant Properties. Catalog*, 1st ed.; Instytut Ochrony Środowiska: Warsaw, Poland, 1991. (In Polish)
30. Moncrieff, J.; Clement, R.; Finnigan, J.; Meyers, T. Averaging, Detrending, and Filtering of Eddy Covariance Time Series. In *Handbook of Micrometeorology: A Guide for Surface Flux Measurement and Analysis*; Atmospheric and Oceanographic Sciences Library; Lee, X., Massman, W., Law, B., Eds.; Springer: Dordrecht, The Netherlands, 2005; pp. 7–31. ISBN 978-1-4020-2265-4.
31. Moncrieff, J.B.; Masheder, J.M.; de Bruin, H.; Elbers, J.; Friborg, T.; Heusinkveld, B.; Kabat, P.; Scott, S.; Soegaard, S.; Verhoef, A. A System to Measure Surface Flux Momentum, Sensible Heat, Water Vapor and Carbon Dioxide. *J. Hydrol.* **1997**, *188–189*, 589–611. [CrossRef]
32. Webb, E.K.; Pearman, G.I.; Leuning, R. Correction of Flux Measurements for Density Effects Due to Heat and Water Vapour Transfer. *Quat. J. R. Met. Soc.* **1980**, *106*, 85–100. [CrossRef]
33. Van Dijk, A.; Moene, A.F.; Debruin, H.A.R. *The Principles of Surface Flux Physics: Theory, Practice and Description of the ECPACK Library*; Internal Report 2004/1; Meteorology and Air Quality Group, Wageningen University: Wageningen, The Netherlands, 2004.
34. Vickers, D.; Mahrt, L. Quality Control and Flux Sampling Problems for Tower and Aircraft Data. *J. Atmos. Oceanic Technol.* **1997**, *14*, 512–526. [CrossRef]
35. Kljun, N.; Calanca, P.; Rotach, M.W.; Schmid, H.P. A Simple Parameterisation for Flux Footprint Predictions. *Bound.-Layer Meteorol.* **2004**, *112*, 503–523. [CrossRef]
36. Egnér, H.; Riehm, H.; Domingo, W.R. Studies on Chemical Soil Analysis as a Basis for Assessing the Nutrient Status of Soils. II. Chemical Extraction Methods for Phosphorus and Potassium Determination. *Kungliga Lantbrukshögskolans Annaler* **1960**, *26*, 199–215. (In German)
37. du Plessis, J. *Maize Production*, 1st ed.; Department of Agriculture, Republic of South Africa: Pretoria, South Africa, 2003.
38. Rutkowski, J. *Technology of Maize Cultivation–From Sowing to Harvesting*, 1st ed.; Warmińsko-Mazurski Ośrodek Doradztwa Rolniczego: Olsztyn, Poland, 2018. (In Polish)
39. Kaniuczak, Z.; Pruszyński, S. *Methodology of Integrated Maize Production*, 3rd ed.; Główny Inspektorat Ochrony Roślin i Nasiennictwa: Warsaw, Poland, 2020. (In Polish)
40. Cofas, E. The Dynamics of Maize Production in the Climate Factors Variability Conditions. In Proceedings of the Agrarian Economy and Rural Development–Realities and Perspectives for Romania, 9th Edition of the International Symposium, Bucharest, Bucharest, 20–21 November 2018; The Research Institute for Agricultural Economy and Rural Development (ICEADR): Bucharest, Bucharest, 2018; pp. 239–245.
41. Lino, A.C.M.; Buzetti, S.; Teixeira Filho, M.C.M.; Galindo, F.S.; Maestrelo, P.R.; Rodrigues, M.A.D.C. Effect of Phosphorus Applied as Monoammonium Phosphate-Coated Polymers in Corn Culture under No-Tillage System. *Semin. Ciências Agrárias SCA* **2018**, *39*, 99. [CrossRef]
42. Pereira, N.C.M.; Galindo, F.S.; Gazola, R.P.D.; Dupas, E.; Rosa, P.A.L.; Mortinho, E.S.; Filho, M.C.M.T. Corn Yield and Phosphorus Use Efficiency Response to Phosphorus Rates Associated With Plant Growth Promoting Bacteria. *Front. Environ. Sci.* **2020**, *8*, 40. [CrossRef]
43. Pettigrew, W.T. Potassium Influences on Yield and Quality Production for Maize, Wheat, Soybean and Cotton. *Physiol. Plant.* **2008**, *133*, 670–681. [CrossRef] [PubMed]
44. Madar, R.; Singh, Y.V.; Meena, M.C.; Das, T.K.; Gaind, S.; Verma, R.K. Potassium and Residue Management Options to Enhance Productivity and Soil Quality in Zero Till Maize–Wheat Rotation. *Clean–Soil Air Water* **2020**, *48*, 1900316. [CrossRef]
45. Niu, J.; Zhang, W.; Chen, X.; Li, C.; Zhang, F.; Jiang, L.; Liu, Z.; Xiao, K.; Assaraf, M.; Imas, P. Potassium Fertilization on Maize under Different Production Practices in the North China Plain. *Agron. J.* **2011**, *103*, 822–829. [CrossRef]
46. Sacks, W.J.; Deryng, D.; Foley, J.A.; Ramankutty, N. Crop Planting Dates: An Analysis of Global Patterns: Global Crop Planting Dates. *Glob. Ecol. Biogeog.* **2010**, *19*, 607–620. [CrossRef]
47. Horoszkiewicz-Janka, J.; Korbas, M.; Mrówczyński, M. *Methodology of Integrated Protection of Winter and Spring Wheat for Producers*, 1st ed.; Instytut Ochrony Roślin Państwowy Instytut Badawczy: Poznań, Poland, 2013. (In Polish)
48. Tomicka, I.; Bujnowska, Z. *Crop Production*, 2nd ed.; Państwowe Wydawnictwa Rolnicze i Leśne: Warsaw, Poland, 1995; Volume 2. (In Polish)

49. Nleya, T. Chapter 4: Winter Wheat Planting Guide. Available online: https://extension.sdstate.edu/igrow-wheat-best-management-practices-wheat-production (accessed on 28 December 2022).
50. Zając, T.; Klimek-Kopyra, A.; Oleksy, A.; Lorenc-Kozik, A.; Ratajczak, K. Analysis of Yield and Plant Traits of Oilseed Rape (Brassica Napus L.) Cultivated in Temperate Region in Light of the Possibilities of Sowing in Arid Areas. *Acta Agrobot.* **2016**, *69*, 1–13. [CrossRef]
51. Pospišil, M.; Brčić, M.; Husnjak, S. Suitability of Soil and Climate for Oilseed Rape Production in the Republic of Croatia. *Agric. Conspec. Sci.* **2011**, *76*, 35–39.
52. Ray, R.L.; Griffin, R.W.; Fares, A.; Elhassan, A.; Awal, R.; Woldesenbet, S.; Risch, E. Soil CO_2 Emission in Response to Organic Amendments, Temperature, and Rainfall. *Sci. Rep.* **2020**, *10*, 5849. [CrossRef]
53. Liu, C.; Wu, Z.; Hu, Z.; Yin, N.; Islam, A.R.M.T.; Wei, Z. Characteristics and Influencing Factors of Carbon Fluxes in Winter Wheat Fields under Elevated CO_2 Concentration. *Environ. Pollut.* **2022**, *307*, 119480. [CrossRef] [PubMed]
54. Paustian, K.; Six, J.; Elliott, E.T.; Hunt, H.W. Management Options for Reducing CO_2 Emissions from Agricultural Soils. *Biogeochemistry* **2000**, *48*, 147–163. [CrossRef]
55. Xu, L.; Baldocchi, D.D. Seasonal Variation in Carbon Dioxide Exchange over a Mediterranean Annual Grassland in California. *Agric. For. Meteorol.* **2004**, *123*, 79–96. [CrossRef]
56. Jans, W.W.P.; Jacobs, C.M.J.; Kruijt, B.; Elbers, J.A.; Barendse, S.; Moors, E.J. Carbon Exchange of a Maize (Zea Mays L.) Crop: Influence of Phenology. *Agric. Ecosys. Environ.* **2010**, *139*, 316–324. [CrossRef]
57. Wang, W.; Liao, Y.; Wen, X.; Guo, Q. Dynamics of CO2 Fluxes and Environmental Responses in the Rain-Fed Winter Wheat Ecosystem of the Loess Plateau. *China. Sci. Total Environ.* **2013**, *461–462*, 10–18. [CrossRef] [PubMed]
58. Eshonkulov, R.A. Turbulent Exchange of Energy, Water and Carbon between Crop Canopies and the Atmosphere: An Evaluation of Multi-Year, Multi-Site Eddy Covariance Data. Ph.D. Thesis, University of Hohenheim, Stuttgart, Germany, 21 March 2019.
59. Zhang, L.; Sun, R.; Xu, Z.; Qiao, C.; Jiang, G. Diurnal and Seasonal Variations in Carbon Dioxide Exchange in Ecosystems in the Zhangye Oasis Area, Northwest China. *PLoS ONE* **2015**, *10*, e0120660. [CrossRef]
60. Li, X.; Liu, L.; Yang, H.; Li, Y. Relationships between Carbon Fluxes and Environmental Factors in a Drip-Irrigated, Film-Mulched Cotton Field in Arid Region. *PLoS ONE* **2018**, *13*, e0192467. [CrossRef]